

Research Article

Effect of the Material Parameters on Layered Viscoelastic Frictional Contact Systems

Fatin F. Mahmoud, Ahmed G. El-Shafei, Amal E. Al-Shorbagy, and Alaa A. Abdel Rahman

Department of Mechanical Engineering, College of Engineering, Zagazig University, Zagazig 44511, Egypt

Correspondence should be addressed to Alaa A. Abdel Rahman, alaa_abouahmed@yahoo.com

Received 12 November 2009; Revised 19 March 2010; Accepted 29 March 2010

Academic Editor: Arvind Agarwal

Copyright © 2010 Fatin F. Mahmoud et al. This is an open access article distributed under the Creative Commons Attribution License, which permits unrestricted use, distribution, and reproduction in any medium, provided the original work is properly cited.

In the design process, one of the main targets is to reduce the peak values of the contact stresses. This can be attained by layering the contacting bodies by layers of different material characteristics. Viscoelastic materials are characterized by either a stress relaxation or a creep deformation; therefore, the contacting bodies can be layered with such materials to attain this target. This paper discusses effects of the material characteristics of viscoelastic layers upon the unbounded contact configuration. Three material parameters are considered: the layer/contact solids stiffness ratio, the delayed/instantaneous elasticity ratio, and the material relaxation time. The results are obtained by using a two-dimensional time-dependent nonlinear computational model, developed by the authors, capable of analyzing quasistatic viscoelastic frictional contact problems.

1. Introduction

Many mechanical applications involve solid bodies coming into contact under the action of applied loads. Upon loading, both normal and tangential contact stresses built up throughout the contact interfaces. These contact stresses have a vital role on the tribological behavior of the contact systems. In the design process, one of the main targets is to reduce the peak values of these contact stresses. Based on the function of the contact system and due to the nature of the viscoelastic materials, layering the contacting bodies by viscoelastic layers with different material properties can attain this target.

Many achievements have been developed to model the linear behavior of viscoelastic materials. Hopkins and Hamming [1] studied the interrelation of the uniaxial creep compliance and the relaxation modulus by using the finite difference method. Lee and Rogers [2] integrated the Volterra type integrals that arise in viscoelastic stress analysis problems using a step-by-step scheme. Taylor and Chang [3] developed an axisymmetric FE model for thermo-rheologically simple materials based on the virtual work principle to derive the constitutive equations. All these developed procedures included no recursive relations, and so they

are limited to problems with only a few degrees-of-freedom. This shortcoming is overcome by Taylor et al. [4] who devised a recursive form of the constitutive relationships. On the other hand, a direct incremental formulation of the constitutive equations for orthotropic linear viscoelastic material is presented by Zocher [5] and Zocher et al. [6], while Dirichlet's series is adopted by Jurkiewicz et al. [7] to incrementalize the constitutive equations.

Contact of viscoelastic bodies, with or without friction, involves many achievements. Chen et al. [8] established a generalized Maxwell FE model for the analysis of linear viscoelastic contact problems with friction. Based on the developed incremental relaxation procedure, the total stress at any instant is found to be dependent on the past stress history and the incremental strain. With the classical Coulomb's law of friction, Rochdi et al. [9] proved the existence of a unique weak solution for the quasistatic problem of frictional contact between a deformable body and a rigid foundation. The material was assumed to have a nonlinear viscoelastic behavior. The contact is modeled with normal compliance. Based on a nonlocal version of Coulomb's law of friction, Shillor and Sofonea [10] presented a weak formulation for the problem of bilateral frictional contact of a nonlinear viscoelastic body with an obstacle.

Awbi et al. [11] formulated a nonlinear abstract evolution problem describing a class of frictional contact problem between a viscoelastic body and a foundation. The problem is set as a time dependent differential inclusion. Han and Sofonea [12] considered a class of evolutionary variational inequalities arising in the frictional contact problems for viscoelastic materials. Awabi et al. [13] extended the study of Shillor and Sofonea [10] to include the quasistatic bilateral viscoelastic frictional contact conditions with a more general friction law. In a comprehensive analysis, Han and Sofonea [14] presented three distinct formulations for viscoelastic frictional contact problems. In the first formulation, the contact is bilateral with a slip dependent friction, and in the second one, the contact is modeled with a normal compliance with a general version of Coulomb's law, while in the third formulation, the contact is described by a general normal damped response condition with a related version of Coulomb's law. In all formulations, both classical and variational formulations are presented. Campo et al. [15] studied a quasistatic viscoelastic frictional contact problem using the classical tresca's law of friction. The effect of damage is included into the model and a fully discrete scheme using the FEM and Euler scheme is introduced. Mahmoud et al. [16] developed an incremental FE model to analyze frictionless viscoelastic contact problems. The model adopted the Wiechert model to simulate the linear response of viscoelastic materials and the incremental convex programming method to manipulate contact events. This model is then extended to handle the frictional contact problems [17].

Mathematical modeling of the friction throughout the contact interface based on the classical theories of friction leads to both physical and mathematical infeasibilities [18]. Physically, classical friction law is only capable of modeling friction between two rigid bodies, while mathematically, the normal contact pressure is ill defined. To overcome unrealistic simulation of the friction throughout the contact interface, several friction theories have been proposed in the last five decades to explain the nature of dry friction between surfaces of deformable bodies in contact. The most realistic friction model is proposed by Bowden and Tabor [19] that known as the welding, shearing, and ploughing theory. According to the welding, shearing, and ploughing theory, the friction force is attributed to two components: the adhesion component and the deformation component. For rough engineering surfaces, the adhesion effect can be neglected, Tworzydlo et al. [20]. The welding, shearing, and ploughing theory is the basis for the nonclassical friction laws. Nonclassical nonlocal-nonlinear friction models are developed by many researchers, among of them Oden and Pires [21, 22].

Analytical and numerical models studying the layering effect upon the contact configuration have been developed for either elastic or viscoelastic layer. Analytically, solutions for contact stresses and deformations in both thin and thick elastic layers are obtained by Johnson [23], Jaffar [24], Barber [25], and Teodorescu et al. [26], as well as for viscoelastic layer, Naghieh et al. [27, 28]. These approaches are efficient, but restricted to certain layer thickness or contact geometry.

Therefore, for most cases one needs to turn to numerical methods. Jaffar [29] has numerically investigated the contact problem of an elastic layer and a sinusoidally rigid indenter. The effect of friction is investigated by using the classical Coulomb's law of friction [30]. The analysis is extended to handle the problem of free rolling with two limiting cases: full slip and fully stick over the entire contact area [31]. These investigations showed that the compressibility of the elastic layer has a great effect on both the surface roughness of the indenter and on the deformation outside the contact area, particularly close to the contact ends. Naghieh et al. [28] extended their work [27] to present the FE analysis for thin layered elastic and viscoelastic solids in contact with rigid substrates. Comparison of the computational results with the analytical ones showed a significant divergence. This divergence is attributed to the modeling of the thin layer as a half-space. Goryacheva and Saseghi [32] investigated the frictional rolling and sliding contacts of an elastic cylinder and a layered foundation. The foundation is modeled as a 2D elastic half-space. The 1D Maxwell model is used to describe the normal and tangential compliance of the viscoelastic layer. Results showed that the contact status depends on the load, velocity, geometrical, and mechanical properties of the contacting bodies. Moreover, the distribution and size of the slip and no-slip contact zones are determined for different values of viscoelastic properties and sliding friction coefficients. Goryacheva et al. [33] extended the analysis to investigate the effect of viscoelastic layer on pressure, film thickness, and friction coefficient in lubricated contacts. Xiao et al. [34] used the superelastic rubber, with large deformation, to design a covering-layer structure of driving drum surface of belt conveyor. The stress and deformation states of driving drums including superelastic rubber and common covering-layer are obtained by FE static intensity analysis using ANSYS.

This paper presents numerical results showing effects of the viscoelastic layer characteristics upon the contact configuration. Three material parameters will be considered: the layer/contact solid stiffness ratio E_{eqv}/E_c , the delayed/instantaneous elasticity ratio E_1/E_∞ , and the material relaxation time of the layer ρ . The results are obtained by using a two-dimensional time-dependent nonlinear FE model, developed by Mahmoud et al. [16, 17], that modified to account for the layering effect. The model adopts the Wiechert model, presented by Williams [35], to simulate the linear response of viscoelastic materials. The resulting constitutive equations, which have an integral form, are reformulated into an incremented form [6] suitable for the FE calculations. The incremental convex programming method with Lagrange multipliers, developed by Hassan and Mahmoud [36], is utilized and modified to accommodate the viscoelastic frictional contact problems. To avoid the drawbacks associated with the classical friction laws, the welding, shearing, and ploughing theory is adopted, and a local nonlinear friction model is developed. To express frictional resistance at the microslip contact zones, a tangential stiffness is added to the overall stiffness of the system.

2. Statement of the Problem

Consider that the two deformable bodies covered by viscoelastic layers, shown in Figure 1, are pressed together by an external normal load F_n and subject to a tangential load F_t . The materials of the contacting bodies may be elastic, viscoelastic or even rigid. Layers are assumed to be perfectly bonded to the contacting bodies. Under such loading condition, it is assumed that the rolling of one body relative to the other is prevented. Assume that each of the contacting bodies occupies a bounded domain Ω in R^N , $N \leq 3$. The boundary Γ is consisted of three disjoint measurable parts: Γ_d , Γ_f , and Γ_c . Γ_d , Γ_f , are portions of the boundary on which displacement and traction are prescribed, respectively. Γ_c is the candidate contact zone containing the adjacent surfaces, which may come into contact upon the application of loads.

With the application of load, the boundary conditions on the contact interface change continuously. Therefore, the contact region advances or recedes according to the type of contact [37]. Moreover, due to the friction effect, the boundary portion Γ_c may be decomposed into two regions: the microslip and the macroslip. For such types of problems, the time-dependent contact status depends on the applied load, geometry, and relative material compliance of both bodies and layers. Such problems belong to a class of nonlinear variational initial boundary value problems having inequality types of constraints. Neglecting the inertia term, a quasistatic problem is defined by the following model:

$$\begin{aligned} \sigma_{ji,j} + f_i &= 0 \quad (\text{in } \Omega), \\ u_i &= 0 \quad (\text{on } \Gamma_d), \\ F_{ii} &= \sigma_{ji}n_j \quad (\text{on } \Gamma_f), \end{aligned} \quad (1)$$

where σ_{ji} are the stress tensor, f_i refers to the body force per unit volume, u_i is the displacement, and n_j is the normal vector to Γ_f .

The elastic material is assumed to obey Hooke's law. On the other hand, the constitutive relationship for a linear homogeneous nonaging and isothermal viscoelastic material can be expressed as [38]

$$\sigma_{ij}(x, t) = \int_0^t C_{ijkl}(t - t') \frac{\partial \varepsilon_{kl}(x, t')}{\partial t'} dt' \quad (\text{in } \Omega), \quad (2)$$

where C_{ijkl} and ε_{kl} are the fourth-order relaxation modulus and the second-order strain tensors, respectively.

To complete the description of the problem, the boundary conditions throughout the contact interface should be stated. Considering friction, the welding, shearing, and ploughing theory [39] is adopted to present a more realistic and reliable friction model. According to this theory, the frictional stress is composed of two components: adhesion and grooving components. For rough engineering surfaces, the adhesion effect can be neglected [20]. Moreover, the contact interface is composed of two zones: microslip and macroslip zones. In the microslip contact zone the tangential contact traction is below the friction capacity. The frictional

capacity depends on the induced contact pressure, the coefficient of friction, and a certain measure of the welded junction stiffness. On the other hand, in the macroslip contact zone, that corresponds to the full sliding state, the tangential load reaches the friction capacity at the contact interface. Variation of the tangential contact stress with the relative tangential displacement is illustrated in Figure 2.

According to Oden and Pires [21], the nonlinear relation between the frictional stress and the relative tangential displacement throughout the contact interface can be represented as

$$\tilde{\sigma}_T = -\mu|\sigma_n|\Phi_\varepsilon(|\tilde{u}_T|) \frac{\tilde{u}_T}{|\tilde{u}_T|}, \quad (3)$$

where $\tilde{\sigma}_T$ is the tangential contact stress vector, σ_n is the normal contact stress, \tilde{u}_T is the relative tangential displacement vector, μ is the static coefficient of friction, ε is a positive parameter that used as a measure to the stiffness of the welded junction, and Φ_ε is a nonlinear, continuous, and real-valued function which can be defined by many forms of functions [21]; one of these functions can be defined as follows

$$\Phi_\varepsilon(|\tilde{u}_T|) = \begin{cases} \frac{|\tilde{u}_T|}{\varepsilon} & \text{if } |\tilde{u}_T| \leq \varepsilon \text{ (microslip level)}, \\ 1 & \text{if } |\tilde{u}_T| > \varepsilon \text{ (macroslip level)}. \end{cases} \quad (4)$$

It is noticed that as ε tends to zero, the local-nonlinear friction model, defined by (3) and (4), will turn to the classical Coulomb's law. Therefore, for frictional contact, the following contact conditions must be imposed throughout the contact interface Γ_c :

$$\begin{aligned} u_n - G &\leq 0, & u_n &= (u_i^1 - u_i^2) \cdot n_j, \\ \sigma_n &= \sigma_{ij}n_i n_j \leq 0, & & \\ \sigma_n \cdot (u_n - G) &= 0, & & \text{(on } \Gamma_c\text{)}, \\ \sigma_{Ti} &= \sigma_{ij}n_j - \sigma_n n_i = -\mu|\sigma_n|\Phi_\varepsilon(|u_{Ti}|) \frac{u_{Ti}}{|u_{Ti}|}, & & \end{aligned} \quad (5)$$

where σ_n is the contact pressure, σ_T is the tangential contact stress, n_j is the outward normal vector to the boundary, u_n is the relative normal displacement, which is a function of the displacements u_i^1 and u_i^2 of the first and second bodies, respectively, at the contact interface, G is the current gap measured along the outward normal vector, and superscripts 1 and 2 denote the first and second body, respectively.

3. The Computational Model

In this section, the computational model simulating 2D nonlinear quasistatic viscoelastic frictional contact problems will be briefly outlined. All ingredients, modules and solution procedure of the model are presented in [16, 17]. In the general framework of the FEM, the space domain of the contact system is discretized into finite elements.

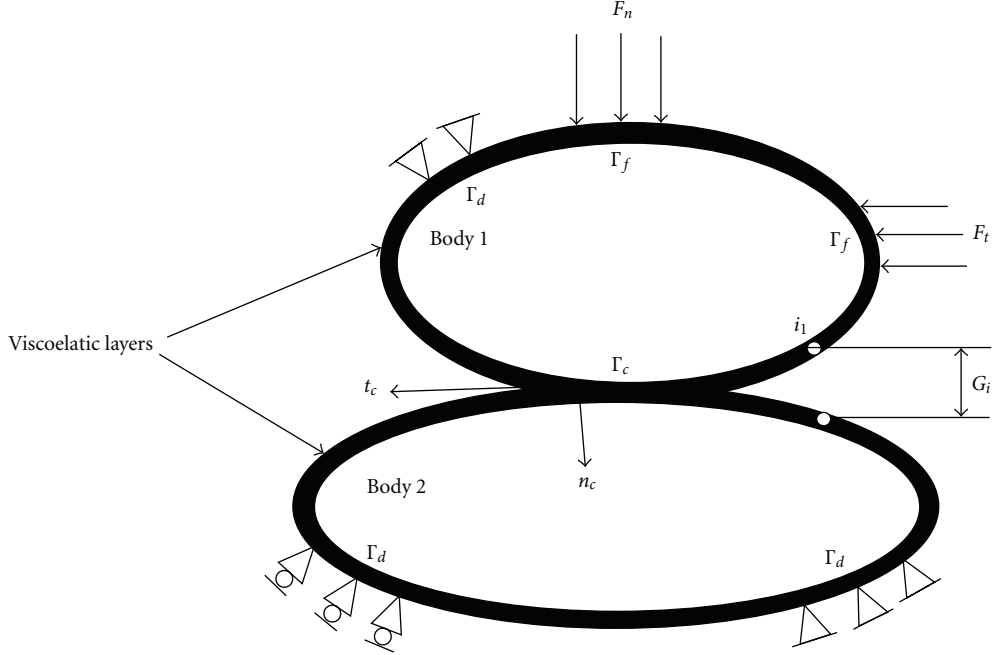
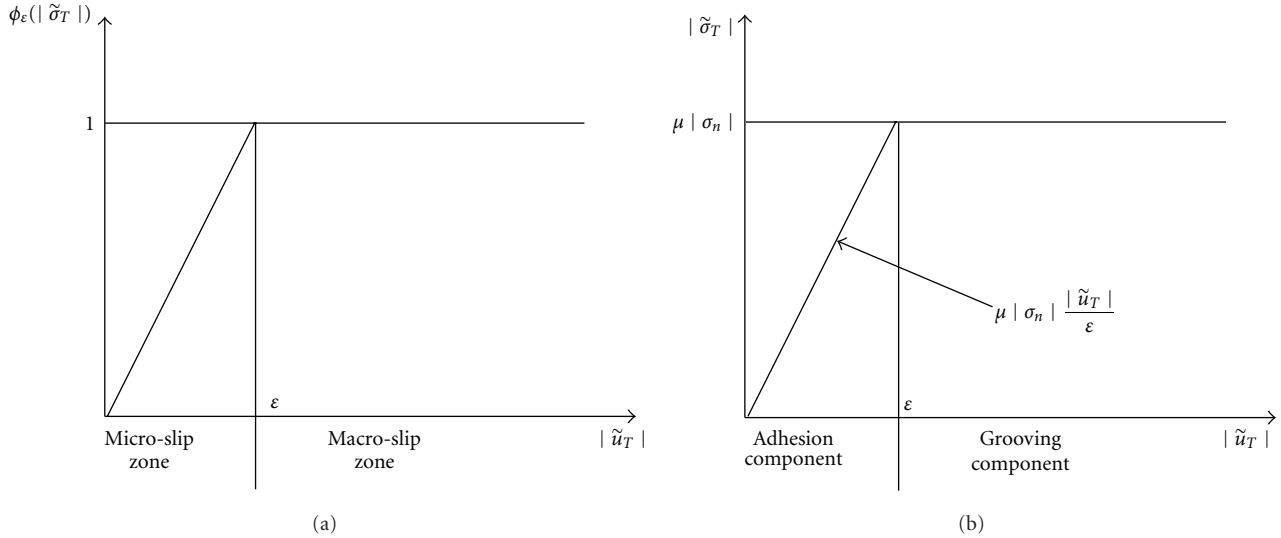


FIGURE 1: Contact of two-layered deformable bodies.

FIGURE 2: (a) Nonlinear function of Φ_ε and (b) variation of the tangential contact stress.

Element equations are evaluated by using Gauss-quadrature integration scheme [40]. The time domain is also discretized into time steps. In each time step, a set of increments is performed to obtain the equilibrium contact configuration corresponding to that time step.

The solution procedure for each increment consists of five modules. The first one is the construction and solution of the overall equilibrium equations, considering the contact constraints, to obtain the incremental displacement and normal contact force vectors. In this module, an incremental form of the constitutive equations for viscoelastic materials, suitable for FE analysis, is developed. Based on the local

nonlinear friction model, the tangential contact stiffness representing the frictional resistance within the micro-slip contact zones is calculated and inserted into the global equilibrium equations. The second module is concerned with the application of the incremental convex programming method to detect the contact event and the corresponding scale factor [36]. Based on such scale factor, the third module is devoted to the calculation of the incremental and updating variables: total displacement, relative displacement, normal contact force, and tangential contact force vectors. Further, in this module, the active and inactive constraints sets and its new cardinalities are also updated. The fourth module

calculates the internal stresses considering the damping effect for viscoelastic materials. Finally, the fifth module directs the continuation of the computations. The computations may be continued in three distinct directions. If there is a possibility for the existence of a new contact event at the current time step, a new increment is initiated. On the other hand, if the current load corresponding to the current time step is completely consumed or no new contact event is detected, a new time step is initiated. Finally, if the total load is completely consumed, the computations are terminated. The solution procedure assumes that the response of the contact system is completely known at time t and, $j - 1$ increments have been performed to obtain the solution at time $t + \Delta t$. Also, within the time step Δt , Δt_c^{j-1} is the elapsed time and Δt_r^j is the remaining time, such that $\Delta t = \Delta t_c^{j-1} + \Delta t_r^j$. Prior to the presentation of these modules, the modeling of the contact interface should be clarified.

To model the contact interface, the node-to-segment contact approach, Wriggers [18], is adopted. In this approach one body is assumed to be a contactor while the other is a target. The contact interface is composed of contactor nodes that are candidates to come into contact with the target segments. The contactor nodes should not penetrate the target segments. The nonpenetration condition, defined by the first inequality condition of (5), is tested for each contactor node on the contact interface. A typical situation showing a generic contact set consisting of a contactor node K penetrating a target segment S_l , within the time t , is depicted in Figure 3(a).

To satisfy the nonpenetration condition, the node K should be located at a point P , where P is the physical contact point. The position vector of the contact point P can be expressed in terms of the position vectors of the nodes K_1 and K_2 , which are connecting the target segment S_l using the interpolation shape function. The position vector of the physical contact point P is defined by the parameter ${}^t\xi_P$ [17], such that

$$\begin{aligned} {}^t\xi_P &= \frac{2[({}^tx_{k_1} - {}^tx_{k_2}){}^tx_k + ({}^ty_{k_1} - {}^ty_{k_2}){}^ty_k]}{({}^tx_{k_1} - {}^tx_{k_2})^2 + ({}^ty_{k_1} - {}^ty_{k_2})^2} \\ &\quad - \frac{({}^tx_{k_1}^2 - {}^tx_{k_2}^2) - ({}^ty_{k_1}^2 - {}^ty_{k_2}^2)}{({}^tx_{k_1} - {}^tx_{k_2})^2 + ({}^ty_{k_1} - {}^ty_{k_2})^2}, \end{aligned} \quad (6)$$

where tx_k and ty_k are the Cartesian components of the position vector of the contactor node K . ${}^tx_{k_i}$ and ${}^ty_{k_i}$ are the Cartesian components of the position vectors of the target nodes K_i , where $i = 1, 2$. Based on the equilibrium of this generic contact set, the contact force distributions for the contactor node K and target segment S_l are shown in Figure 3(b).

The direct application of (2) in its form will leads to the requirement of solving of a set of integrals [6]. To avoid evaluation of these integrals, an incremental form of the constitutive equations, which is quite amenable to the implementation in an FE model, is developed. Now, let the considered time domain be subdivided into discrete intervals Δt , such that $t_{n+1} = t_n + \Delta t$. Assuming that the stress state

$\sigma_{ij}(x, t_n)$ is known at time t_n , the stress state $\sigma_{ij}(x, t_{n+1})$ at time t_{n+1} can be expressed as

$$\begin{aligned} \sigma_{ij}(x, t_{n+1}) &= \int_0^{t_n} C_{ijkl}(t_{n+1} - t') \frac{\partial \varepsilon_{kl}(x, t')}{\partial t'} dt' \\ &\quad + \int_{t_n}^{t_{n+1}} C_{ijkl}(t_{n+1} - t') \frac{\partial \varepsilon_{kl}(x, t')}{\partial t'} dt'. \end{aligned} \quad (7)$$

The stress increment from time t_n to time t_{n+1} is defined as

$$\Delta \sigma_{ij} = \Delta \sigma'_{ij} + \Delta \sigma^R_{ij}, \quad (8a)$$

where

$$\begin{aligned} \Delta \sigma'_{ij} &= \int_{t_n}^{t_{n+1}} C_{ijkl}(t_{n+1} - t') \frac{\partial \varepsilon_{kl}(x, t')}{\partial t'} dt', \\ \Delta \sigma^R_{ij} &= \int_0^{t_n} [C_{ijkl}(t_{n+1} - t') - C_{ijkl}(t_n - t')] \frac{\partial \varepsilon_{kl}(x, t')}{\partial t'} dt'. \end{aligned} \quad (8b)$$

Adoption of the Wiechert model, Williams [35], to simulate the linear behavior of viscoelastic materials yields the following definition of the fourth-order relaxation modulus tensor:

$$C_{ijkl}(t_{n+1} - t') = C_{ijkl}^\infty + \sum_{m=1}^M C_{ijkl}^m e^{-((t_{n+1}-t')/\rho_{ijkl}^m)}, \quad (9a)$$

where C_{ijkl}^∞ is the tensor of elastic moduli, M is the number of Maxwell elements used in the Wiechert model, C_{ijkl}^m and η_{ijkl}^m are spring constants and the dashpot coefficients of Maxwell elements respectively, and ρ_{ijkl}^m is the relaxation time of Maxwell elements, defined as

$$\rho_{ijkl}^m = \frac{\eta_{ijkl}^m}{C_{ijkl}^m} \quad (\text{no summation on } i, j, k, l). \quad (9b)$$

Substitution of (9a) and (9b) into (8a) and (8b), with the assumption that the rate of change of the strain within the time step to be constant and then evaluating the integrals yields

$$\Delta \sigma'_{ij} = C'_{ijkl} \Delta \varepsilon_{kl}, \quad \Delta \sigma^R_{ij} = \sum_{m=1}^M (e^{-\Delta t/\rho_{ijkl}^m} - 1) S_{ij}^m(t_n), \quad (10)$$

where

$$C'_{ijkl} = C_{ijkl}^\infty + \frac{1}{\Delta t} \sum_{m=1}^M \eta_{ijkl}^m (1 - e^{-\Delta t/\rho_{ijkl}^m}),$$

$$S_{ij}^m(t_n) = e^{-\Delta t/\rho_{ijkl}^m} S_{ij}^m(t_{n-1}) + \eta_{ijkl}^m \dot{\varepsilon}_{kl}(t_n) (1 - e^{-\Delta t/\rho_{ijkl}^m}). \quad (11)$$

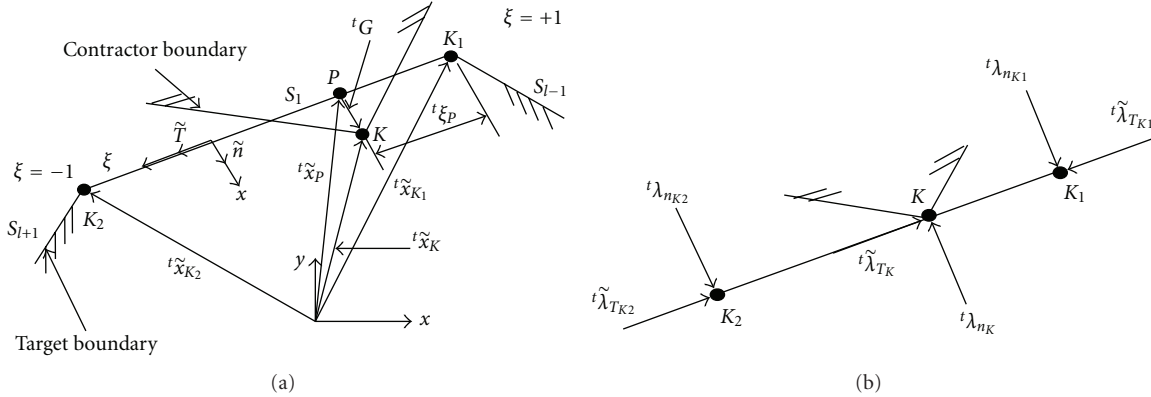


FIGURE 3: Modeling of the contact interface, (a) a contactor node K in contact with a target segment S_l and (b) contact forces at the contact interface.

According to the developed incremental procedure, and for the j th increment, the last four equations can be written in the following matrix form:

$$\begin{aligned} \{\Delta\sigma'\}^j &= {}^{t+\Delta t}[C']^j\{\Delta\varepsilon\}^j, \\ {}^{t+\Delta t}\{\Delta\sigma^R\}^j &= \left\{ \sum_{m=1}^M \left(e^{-\Delta t_c^j/\rho^m} - 1 \right) {}^{t+\Delta t}\{S^m\}^{j-1} \right\}, \\ {}^{t+\Delta t}[C']^j &= [C^\infty] + {}^{t+\Delta t} \left[\frac{1}{\Delta t_r^j} \sum_{m=1}^M [\eta^m] \left(1 - e^{-\Delta t_r^{j-1}/\rho^m} \right) \right], \\ {}^{t+\Delta t}\{S^m\}^j &= e^{-\Delta t_c^j/\rho^m} {}^{t+\Delta t}\{S^m\}^{j-1} \\ &\quad + \left\{ [\eta^m] {}^{t+\Delta t}\{\varepsilon\}^j \left(1 - e^{-\Delta t_c^j/\rho^m} \right) \right\}, \end{aligned} \quad (12)$$

where Δt_c and Δt_r are the consumed and remaining time step, respectively, which can be defined as $\Delta t_c^j = \alpha^j \Delta t$ and $\Delta t_r^j = \Delta t - \Delta t_c^j$ where α^j is the minimum scale factor within the increment j [17].

According to the proposed friction model, the frictional contact force vector in the micro-slip contact zone is defined by (3). This equation can be rewritten in the following form:

$$\tilde{\lambda}_T = -\mu |\tilde{\lambda}_n| \Phi_\epsilon(|\tilde{u}_T|) \frac{\tilde{u}_T}{|\tilde{u}_T|}, \quad (13a)$$

where $\tilde{\lambda}_n$ and $\tilde{\lambda}_T$ are the normal and tangential contact force vectors, respectively. In this zone, the tangential contact force should be compensated by a tangential stiffness. Such stiffness is incorporated into the equilibrium equation of the contact system. According to Mahmoud et al. [41], the tangential contact stiffness due to friction, in the micro-slip contact zone, can be calculated by the differentiation of the tangential force defined by (13a) with respect to the relative displacement; this yields

$$K_T = \frac{d \tilde{\lambda}_T}{d \tilde{u}_T} = \frac{\mu |\lambda_n|}{\varepsilon}. \quad (13b)$$

Based on the spatial discretization of the geometry of the contact interface, illustrated in Figure 3, the tangential contact stiffness located at the contactor node K at the j th increment of time $t + \Delta t$ is defined as

$${}^{t+\Delta t}K_T^j = \frac{\mu |{}^{t+\Delta t}\lambda_{nK}^{j-1}|}{\varepsilon}. \quad (13c)$$

Similarly, the tangential contact stiffness located at the target segment nodes K_1 and K_2 , respectively, at time t is defined as

$$\begin{aligned} {}^{t+\Delta t}K_{T_{K1}}^j &= \frac{\mu |{}^{t+\Delta t}\lambda_{nK1}^{j-1}|}{\varepsilon}, & {}^{t+\Delta t}K_{T_{K2}}^j &= \frac{\mu |{}^{t+\Delta t}\lambda_{nK2}^{j-1}|}{\varepsilon}. \end{aligned} \quad (13d)$$

The contact problem that presented in this paper is defined by a quadratic objective function subject to a set of convex constraints. Therefore, the incremental convex programming method is adopted to handle such type of contact problems. With the incremental convex programming method, the original contact model is transformed into a sequence of constrained submodels. Each one of these submodels has only one additional constraint more than the preceding one. Furthermore, each one of these submodels is manipulated throughout one increment of load. Each additional constraint is corresponding to one possible contact event. Accordingly, the percentage of load that is required for activating or deactivating one constraint is also detected, while the remaining load is applied to the next sub-model. Therefore, the transformation occurs in an incremental adaptive manner such that the total number of increments, or constrained sub-models, does not exceed the number of constraints.

With multiphase frictional contact problems, three contact events are encountered. In the first contact event one potential contact point is currently in separation state (inactive constraint) in the $(j-1)$ th sub-model and candidates to come into contact (active constraint) in the j th sub-model. This means that an advancing contact occurs. The second contact event is concerned with one potential contact point is currently in contact state (active constraint) in the $(j-1)$ th sub-model and candidates to come out of contact

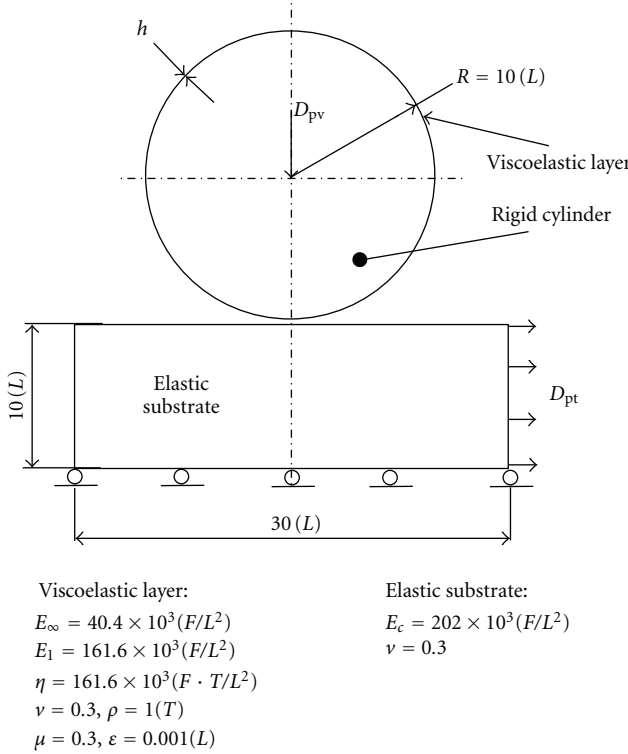


FIGURE 4: Contact of a layered rigid cylinder with an elastic substrate.

(inactive constraint) in the j th sub-model. This implies that a receding contact occurs. The third contact event is encountered due to the existence of friction. In this contact event one potential contact point currently in contact and belonging to the micro-slip contact zone (active constraint) in the $(j-1)$ th sub-model and candidates to transfer to the macro-slip contact zone (active constraint) in the j th sub-model.

All major ingredients of the solution procedure are now clarified; the overall equilibrium equations, considering the contact constraints, can now be written as follows:

$$\begin{aligned} & \begin{pmatrix} [K]^j + [K_T]^{j-1} [C_n]^{j-1} \\ [C_n]^{j-1T} \end{pmatrix} \begin{pmatrix} \{\Delta u\}^j \\ \{\Delta \lambda_n\}^j \end{pmatrix} \\ &= \begin{pmatrix} \{F\}^j + [C_n]^{j-1} \{\lambda_n\}^{j-1} + [C_T]^{j-1} \{\lambda_T\}^{j-1} \\ \{G\}^{j-1} \end{pmatrix}, \end{aligned} \quad (14)$$

in which the matrix operators ${}^{t+\Delta t}[C_n]^{j-1}$ and ${}^{t+\Delta t}[C_T]^{j-1}$ are defined as

$${}^{t+\Delta t}[C_n]^{j-1} = \begin{bmatrix} - {}^{t+\Delta t}\tilde{n}^{j-1T} \\ \left(1 - {}^{t+\Delta t}\xi_k^{j-1}\right) {}^{t+\Delta t}\tilde{n}^{j-1T} \\ \left({}^{t+\Delta t}\xi_k^{j-1}\right) {}^{t+\Delta t}\tilde{n}^{j-1T} \end{bmatrix},$$

$${}^{t+\Delta t}[C_T]^{j-1} = \begin{bmatrix} - {}^{t+\Delta t}\tilde{T}^{j-1T} \\ \left(1 - {}^{t+\Delta t}\xi_k^{j-1}\right) {}^{t+\Delta t}\tilde{T}^{j-1T} \\ \left({}^{t+\Delta t}\xi_k^{j-1}\right) {}^{t+\Delta t}\tilde{T}^{j-1T} \end{bmatrix} \quad (15)$$

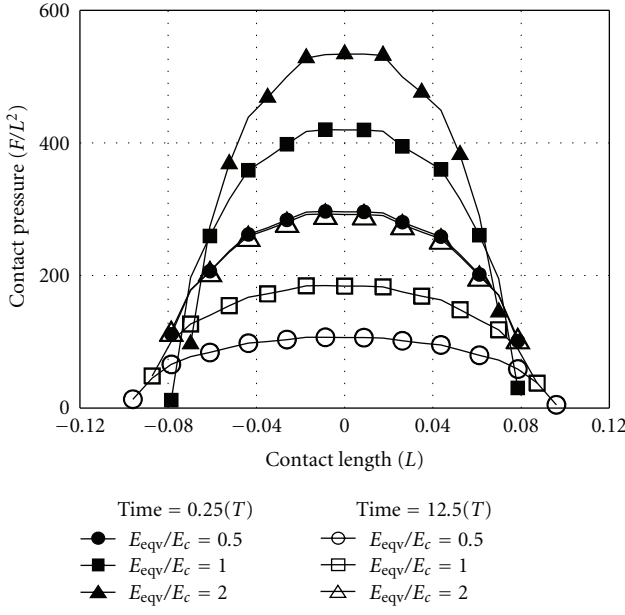
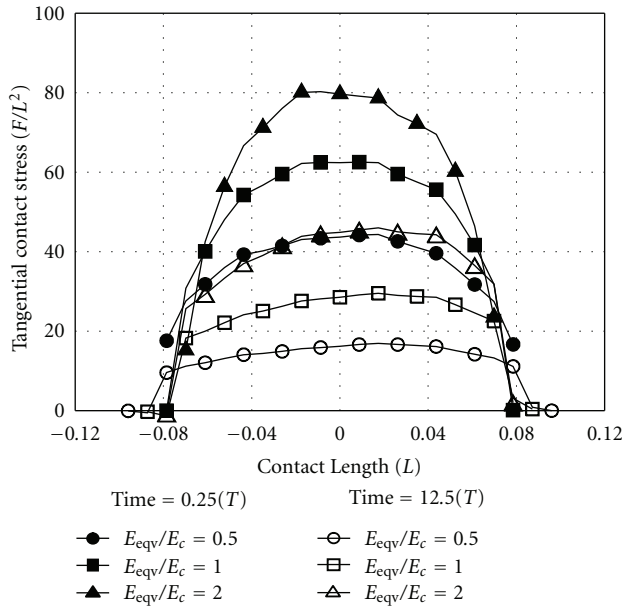
The detailed solution procedure of the two-dimensional time-dependent nonlinear contact model for handling frictional viscoelastic contact problems and its verification are found in [17].

4. Numerical Results

This section is devoted to the presentation and discussion of numerical results of effects of the material characteristics of viscoelastic layers upon the contact configuration. Three material parameters are considered. The first material parameter is the layer/contact solids stiffness ratio E_{eqv}/E_c , where E_{eqv} is the equivalent modulus of the layer, defined by $E_{eqv} = E_\infty + E_1$, and E_c is the modulus of elasticity of the contact solid. The second one is the delayed/instantaneous elasticity modulus ratio of the layer E_1/E_∞ . The last material parameter is the material relaxation time ρ of the layer. For the sake of generality, all results are presented in dimensionless form.

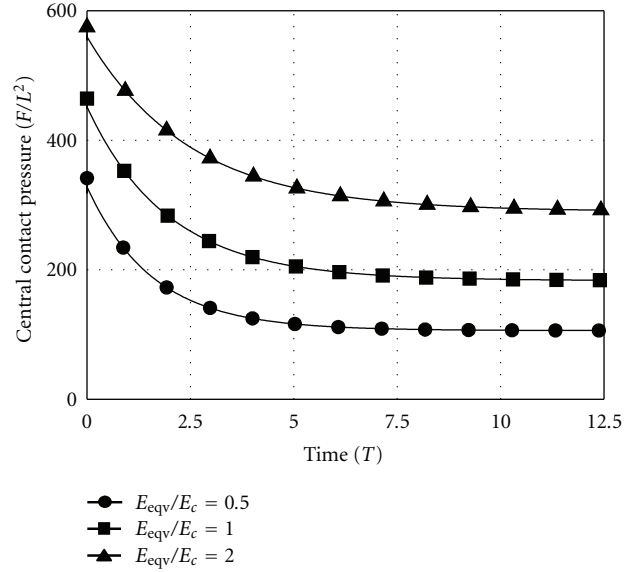
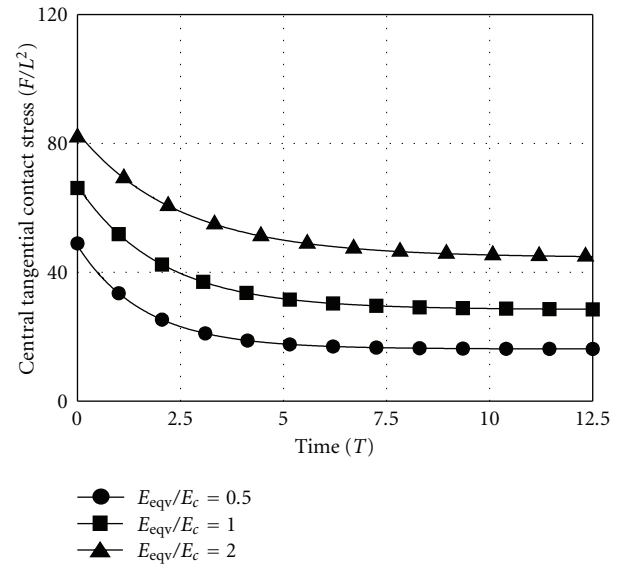
Consider the contact problem of the indentation of an elastic substrate by a nonrolled layered rigid cylinder. The rigid cylinder is covered by a viscoelastic layer which is perfectly bonded to the cylinder. This problem is a plane strain advancing contact problem with a stress relaxation condition. The geometry, material properties, loading, and boundary conditions are shown in Figure 4. The rigid cylinder is subjected to a prescribed uniform vertical displacement D_{pv} of $125 \times 10^{-5} (L)$. The substrate is subjected to a prescribed uniform tangential displacement D_{pt} of $75 \times 10^{-5} (L)$. To satisfy the nonrolling motion, only the rigid cylinder is allowed to move vertically, while prevented from the motion in the horizontal direction. These conditions are not applied to the viscoelastic layer that covered the rigid cylinder. The substrate is made of a linear elastic material, while the viscoelastic material of the layer is simulated by the Wiechert model with a single Maxwell element. The space domain of the problem is modeled by both triangular and four-node quadrilateral finite elements. The FE grid is composed of 885 elements and 938 nodes for the layered rigid cylinder and 1014 elements and 990 nodes for the elastic substrate. The potential contact interface is modeled by 55 candidate nodes, while the time step is 0.025 (T).

4.1. Effect of the Layer/Contact Solid Stiffness (E_{eqv}/E_c). To predict the effect of the layer/contact solid stiffness on the contact configuration, different layer/contact solid stiffness ratios, E_{eqv}/E_c , 0.5 (soft layering) 1.0 and 2.0 (hard layering) are used, where E_c is the modulus of elasticity of the elastic substrata. For all layers, a thickness h of 0.5 (L), relaxation time, ρ of unity, and E_1/E_∞ of 4 are kept constants. Figures 5

FIGURE 5: Effect of E_{eqv}/E_c on the contact pressure distribution.FIGURE 6: Effect of E_{eqv}/E_c on the tangential contact stress distribution.

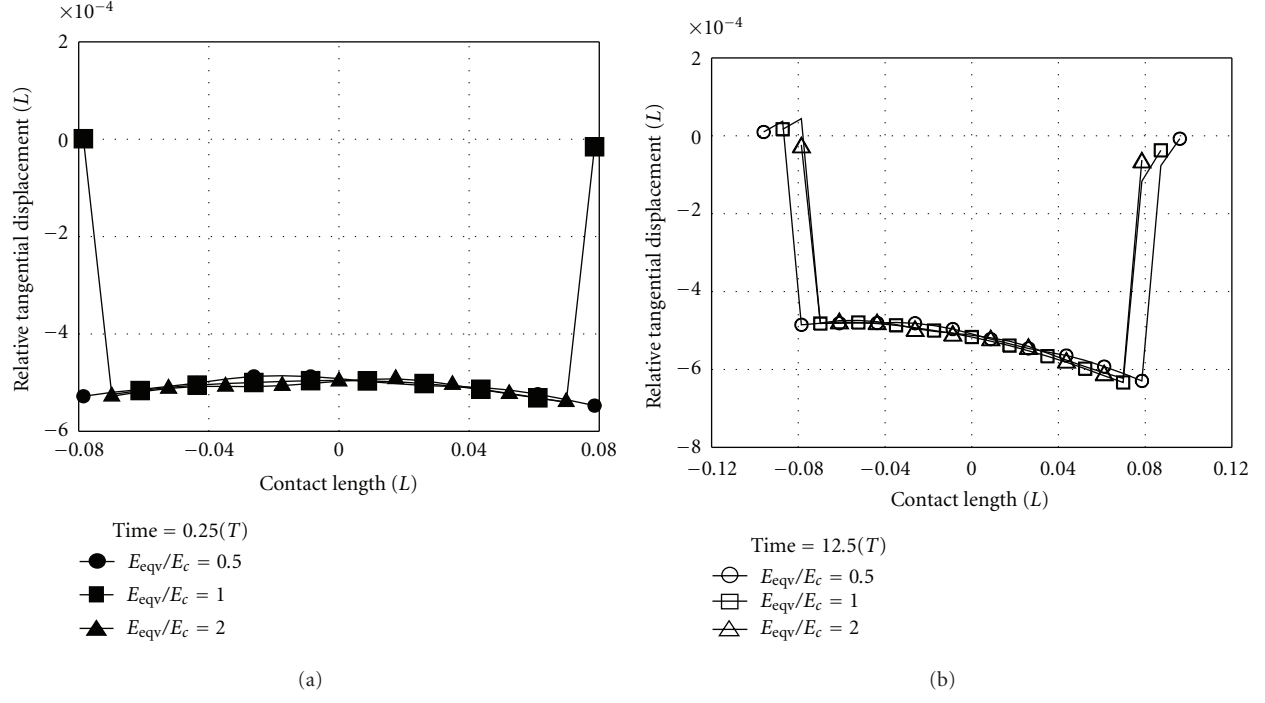
and 6 illustrate the effect of the layer stiffness on both normal and tangential contact stresses distributions, respectively, at different instants of time. With the increasing of the layer stiffness, both normal and tangential contact stresses increase while the contact area decreases. This response is due to the increasing of the stiffness of the contact system. With the time marching and due to the material relaxation, the contact area enlarges and in turn the contact stresses relax.

Figures 7 and 8 display the effect of the layer stiffness on the relaxation rate of the central normal and tangential

FIGURE 7: Effect of E_{eqv}/E_c on relaxation of the central contact pressure.FIGURE 8: Effect of E_{eqv}/E_c on relaxation of the central tangential contact stress.

contact stresses, respectively. It is noticed that as the layer stiffness increases, both the instantaneous and steady-state values of the central contact stress also increase. This behavior is due to the increasing of the stiffness of the contact system. Also, as the layer stiffness decreases, the steady state is reached in a relatively shorter time, that is, using of soft viscoelastic layer accelerates the steady state.

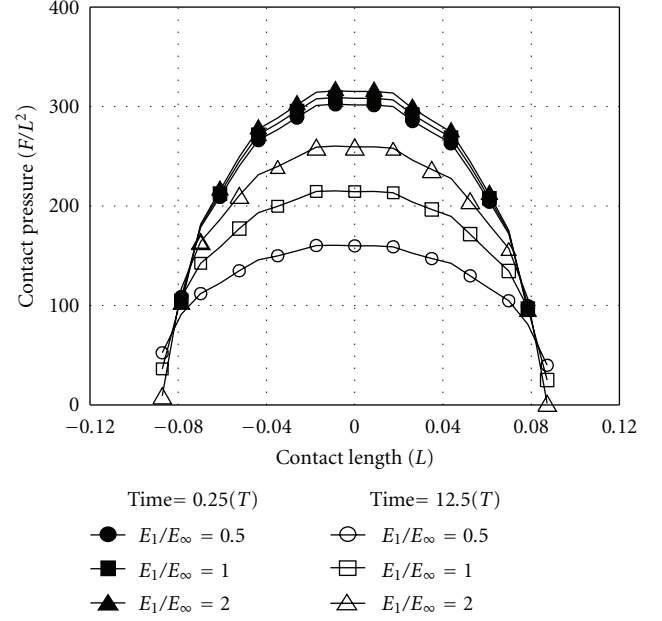
Figure 9 shows the effect of the layer stiffness on the relative tangential displacement at different instants of time. It is clear that, at low time, all the contacting nodes have relative displacements less than the value of the parameter ϵ ; hence all contact nodes are in a micro-slip contact

FIGURE 9: Effect of E_{eqv}/E_c on the relative tangential displacement distribution.

mode. With the time marching, it is found that the relative displacements are slightly increasing, due to the decreasing of the tangential stiffness, but still in the micro-slip contact mode. This implies that there is no significant effect of the layer stiffness on the macro-slip action even with time marching. Although there is no remarkable effect of the layer stiffness on the relative displacement throughout the contact interface, relative displacements and in turn the transition from the micro-slip to macro-slip contact zone are controlled by two factors. The first factor is the parameter ϵ which measures the stiffness of the welded junction in the micro-slip contact zone. This parameter is experimentally measured for any contact system [21]. The second factor is the applied tangential load.

4.2. Effect of the Layer Delayed/Instantaneous Elasticity Moduli Ratio (E_1/E_∞). The effect of the delayed/instantaneous elasticity moduli ratio E_1/E_∞ of the viscoelastic layer on the contact configuration is predicted. Layers with different values of E_1/E_∞ of 0.5, 1.0, and 2.0 are used. For all layers, the relaxation time ρ of unity (T), thickness h of 0.5 (L), and E_{eqv}/E_c of 0.5 (soft layering) are kept constant. Furthermore, the equivalent modulus of the layer $E_{\text{eqv}} = E_1 + E_\infty$ is also kept constant. Figures 10 and 11 illustrate the effect of this ratio on both the normal and tangential contact stresses distributions, respectively, at different instants of time. It is shown that either normal or tangential contact stress increases and the contact area decreases as the ratio E_1/E_∞ increases. With the time marching, both of the contact stresses relax and the contact area slightly increases due to the effect of the material relaxation.

Figures 12 and 13 display the effect of the ratio E_1/E_∞ on the relaxation rate of the central normal and tangential

FIGURE 10: Effect of E_1/E_∞ on the contact pressure distribution.

contact stresses, respectively. It is noticed that there is no effect on the values of the instantaneous contact stresses, while the steady-state values of the stresses increase as E_1/E_∞ increases and the required time to reach it decreases. Furthermore, it is found that the steady state is reached rapidly as the E_1/E_∞ ratio increases; that is, using of viscoelastic layer with high delayed elasticity modulus accelerates the steady-state. Thus, keeping the value of E_{eqv} to be constant the ratio

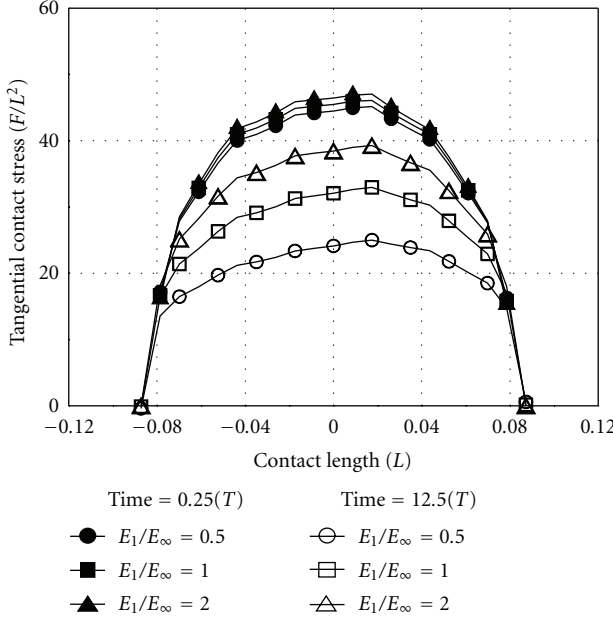


FIGURE 11: Effect of E_1/E_∞ on the tangential contact stress distribution.

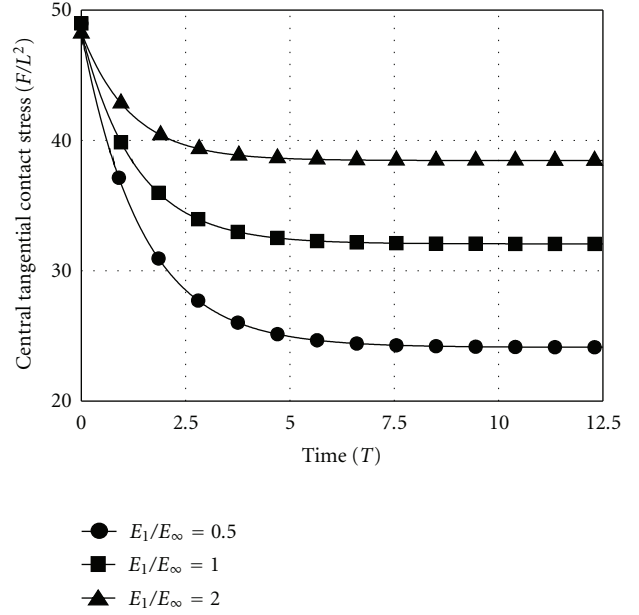


FIGURE 13: Effect of E_1/E_∞ on relaxation of the central tangential contact stress.

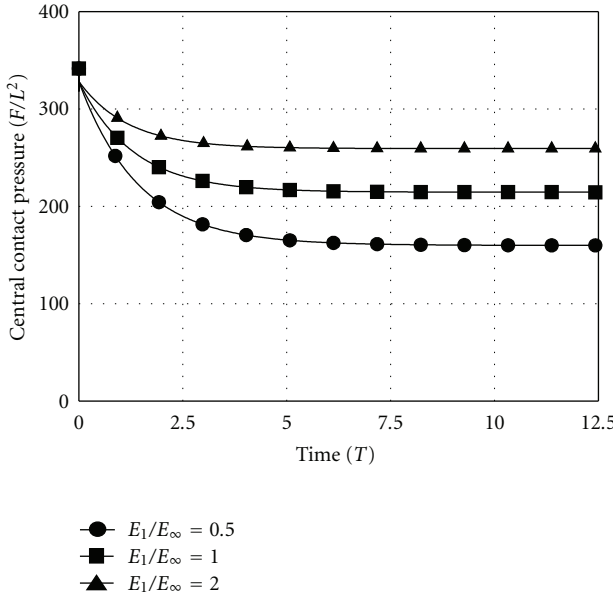


FIGURE 12: Effect of E_1/E_∞ on relaxation of the central contact pressure.

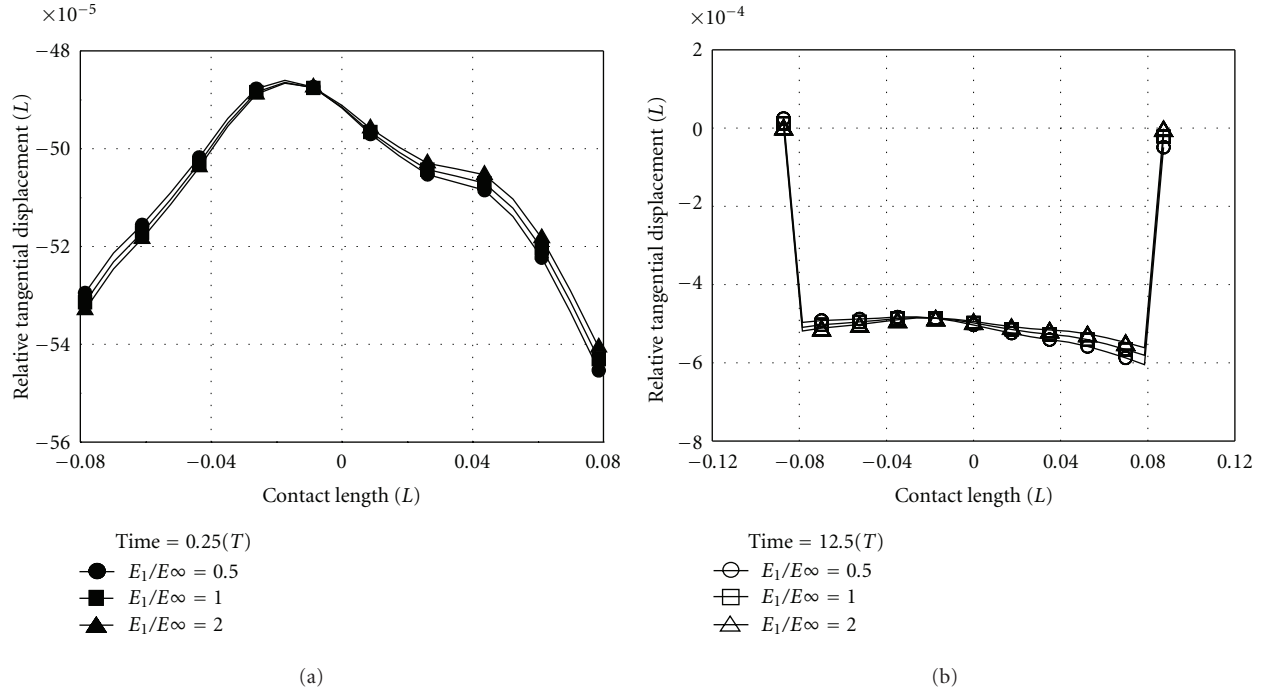
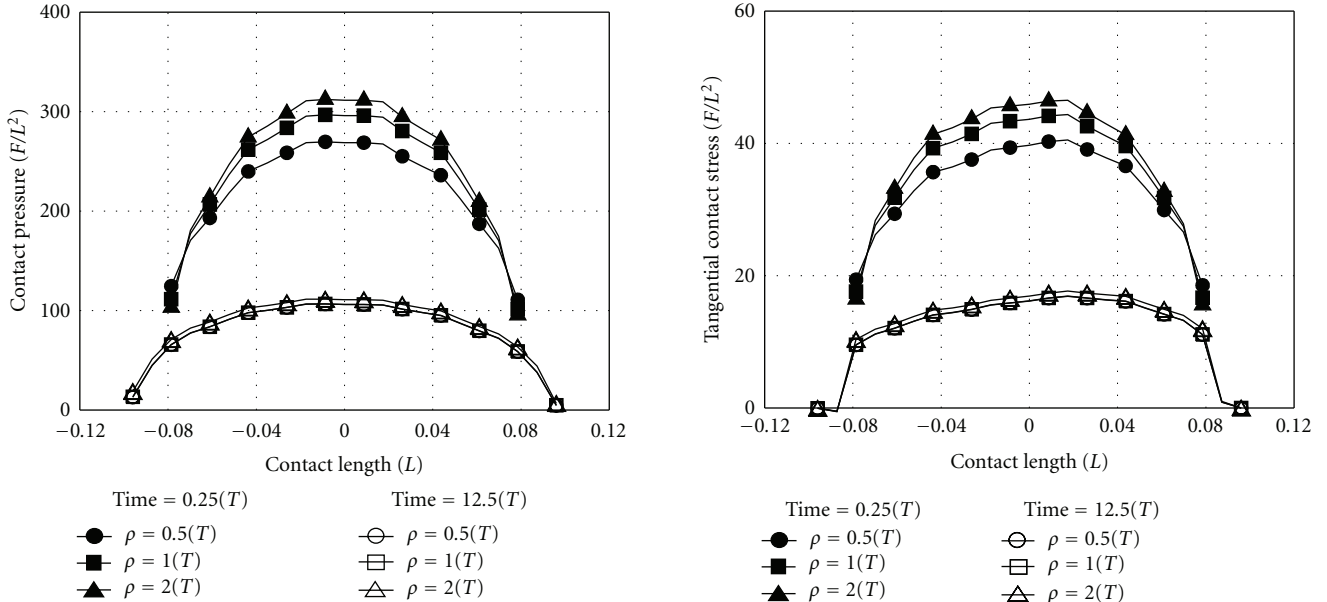
E_1/E_∞ has a remarkable effect on the steady state value of the contact stresses while this effect is vanished at low times.

Figure 14 shows the effect of the ratio E_1/E_∞ on the relative tangential displacement at the contact interface. It is clear that all the contacting nodes are in the micro-slip mode and there is no significant effect of the ratio E_1/E_∞ on the macro-slip action even with time marching.

4.3. Effect of the Layer Relaxation Time (ρ). To predict the effect of the relaxation time of the layer on the contact configuration, layers with different values of relaxation time ρ of 0.5, 1.0, and 2.0(T) are used. For all layers, a thickness of 0.5(L), E_{eqv}/E_c of 0.5 (soft layering), and E_1/E_∞ of 4 are kept constants. Also, all layers have the same value of the delayed modulus of elasticity, E_1 . Hence the variation in the relaxation time depends only on the variation of the viscosity coefficient η . Figures 15 and 16 illustrate the effect of the layer relaxation time on both normal and tangential contact stresses distributions, respectively, at different instants of time. Contact stresses decrease and the contact area increases as the layer relaxation time decreases. With the time marching and due to the material relaxation, both of the contact stresses relax with different rates and the contact area increases.

Figures 17 and 18 show the effect of the layer relaxation time on the relaxation rate of central contact stresses. It is found that there is no effect on the relaxation time of the viscoelastic layer on the instantaneous steady-state values of contact stresses. Only the time required to reach the steady state is increased with the increasing of the relaxation time of the layer. Therefore, using of viscoelastic layer with low relaxation time accelerates the steady state.

Figure 19 shows the effect of the layer relaxation time on the relative tangential displacement at the contact interface at different instants of time. It is clear that the contact interface experiences a micro-slip mode rather than a macro-slip one. Therefore, there is no significant effect of the layer relaxation time on the relative displacements throughout the contact interface.

FIGURE 14: Effect of E_1/E_∞ on the relative tangential displacement distribution.FIGURE 15: Effect of ρ on the contact pressure distribution.FIGURE 16: Effect of ρ on the tangential contact stress distribution.

5. Conclusions

A numerical parametric study has been done to detect effects of the material characteristics of viscoelastic layers, covering the contacting bodies, on the contact configuration. Three material parameters of viscoelastic layers are considered: the layer/contact solid stiffness ratio E_{eqv}/E_c , the delayed/instantaneous elasticity ratio E_1/E_∞ , and the

material relaxation time ρ . Effects of these parameters on the contact configuration as contact stresses distribution, extent of the contact area, relaxation of the contact stresses, and relative tangential displacements throughout the contact interface are completely detected. Effects of the material characteristics of viscoelastic layers on the contact status can be summarized as follows.

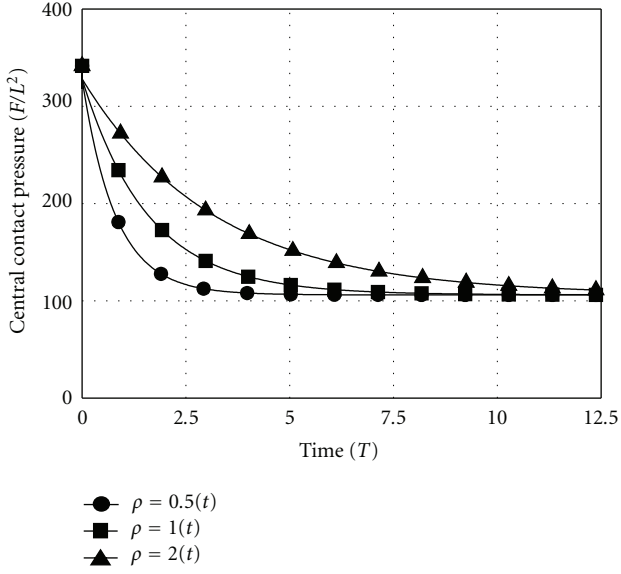


FIGURE 17: Effect of ρ on relaxation of the central contact pressure.

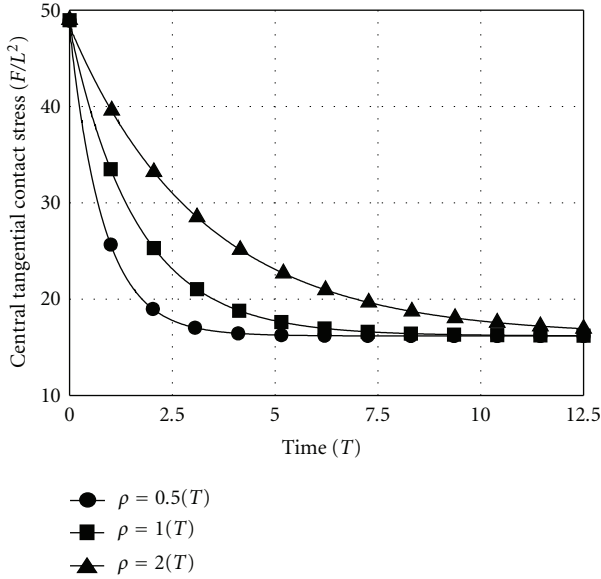
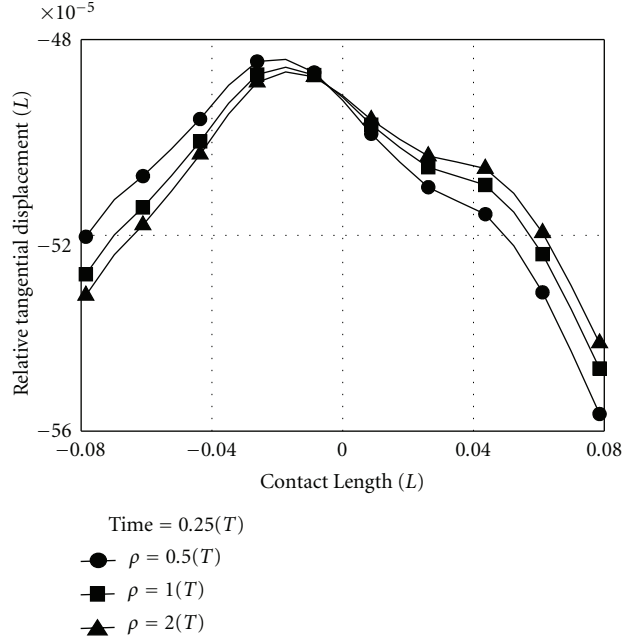
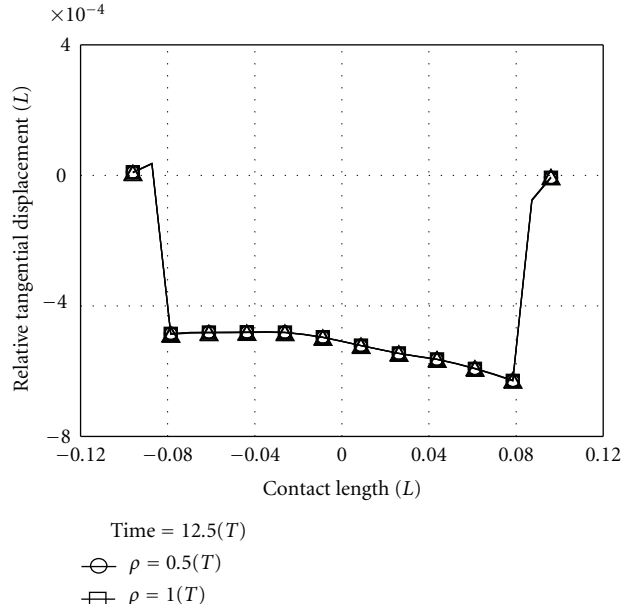


FIGURE 18: Effect of ρ on relaxation of the central tangential contact stress.

Characteristics of viscoelastic layers affect the contact stresses and contact areas significantly. Layering with soft viscoelastic layers ($E_{\text{eqv}}/E_c < 1$) decreases the contact stresses and increasing the contact area. On the other hand, using of hard layers ($E_{\text{eqv}}/E_c > 1$) results in an opposite response. Keeping the equivalent modulus E_{eqv} of the viscoelastic layer to be constant, decreasing the delayed/instantaneous elasticity ratio E_1/E_∞ reduces the contact stresses and increases the contact area. This response is clearly noticed with the time marching. Keeping the instantaneous modulus of elasticity E_1 to be constant, decreasing the relaxation time ρ of the



(a)



(b)

FIGURE 19: Effect of ρ on the relative tangential displacement distribution.

viscoelastic layer reduces the contact stresses and increases the contact area. This response is remarkable at low times.

Relaxation of the contact stresses is influenced by the viscoelastic layer properties. The layer/solid stiffness ratio E_{eqv}/E_c has a significant effect on both instantaneous and steady-state values of contact stresses. Using of soft viscoelastic layers reduces both instantaneous and steady state values of contact stresses. Also, decreasing the ratio E_{eqv}/E_c

accelerates the steady state; that is, with soft viscoelastic layers contact stresses reach their steady-state values more rapidly than with hard layer. Keeping the value of E_{eqv} to be constant, the delayed/instantaneous elasticity ratio E_1/E_∞ has an insignificant effect on the instantaneous value of contact stresses. However, decreasing this ratio reduces the steady-state values of contact stresses. Furthermore, with large values of the ratio E_1/E_∞ the response of the viscoelastic layer approaches the elastic response, and therefore contact stresses reach their steady-state values more rapidly. Keeping the values of E_{eqv} and E_1 to be constant, the layer relaxation time ρ has no effect on effect on both instantaneous and steady-state values of contact stresses. However, with small values of the relaxation time of the layer contact stresses reach their steady state values more rapidly.

The three material properties under consideration E_{eqv}/E_c , E_1/E_∞ , and ρ have insignificant effect on the relative tangential displacement throughout the contact interface. The micro-slip contact mode is dominant; that is, no contact zones experience gross-sliding mode. However, this response is affected by both the applied side load and the parameter ϵ which measures the stiffness of the welded junction in the micro-slip contact zone.

References

- [1] I. L. Hopkins and R. W. Hamming, "On creep and relaxation," *Journal of Applied Physics*, vol. 28, no. 8, pp. 906–909, 1957.
- [2] E. H. Lee and T. G. Rogers, "Solution of viscoelastic stress analysis problems using measured creep or relaxation functions," *Journal of Applied Mechanics*, vol. 30, no. 1, pp. 127–133, 1963.
- [3] R. L. Taylor and T. Y. Chang, "An approximate method for thermoviscoelastic stress analysis," *Nuclear Engineering and Design*, vol. 4, no. 1, pp. 21–28, 1966.
- [4] R. L. Taylor, K. S. Pister, and G. L. Goudreau, "Thermomechanical analysis of viscoelastic solids," *International Journal for Numerical Methods in Engineering*, vol. 2, no. 1, pp. 45–59, 1970.
- [5] M. A. Zocher, *A thermoviscoelastic finite element formulation for the analysis of composites*, Ph.D. dissertation, Texas A & M University, Collage Station, Tex, USA, 1995.
- [6] M. A. Zocher, S. E. Groves, and D. H. Allen, "A three-dimensional finite element formulation for thermoviscoelastic orthotropic media," *International Journal for Numerical Methods in Engineering*, vol. 40, no. 12, pp. 2267–2288, 1997.
- [7] B. Jurkiewicz, J.-F. Destrebecq, and A. Vergne, "Incremental analysis of time-dependent effects in composite structures," *Computers & Structures*, vol. 73, no. 1–5, pp. 425–435, 1999.
- [8] W. H. Chen, C. M. Chang, and J. T. Yeh, "Finite element analysis of viscoelastic contact problems with friction," in *Proceedings of the 15th National Conference on Theoretical and Applied Mechanics*, pp. 713–720, Tainan, Taiwan, 1991.
- [9] M. Rochdi, M. Shillor, and M. Sofonea, "Quasistatic viscoelastic contact with normal compliance and friction," *Journal of Elasticity*, vol. 33, no. 2–3, pp. 105–126, 1998.
- [10] M. Shillor and M. Sofonea, "Quasistatic viscoelastic contact problem with friction," *International Journal of Engineering Science*, vol. 38, no. 14, pp. 1517–1533, 2000.
- [11] B. Awbi, M. Rochdi, and M. Sofonea, "Abstract evolution equations for viscoelastic frictional contact problems," *Journal of Applied Mathematics and Physics*, vol. 51, no. 2, pp. 218–235, 2000.
- [12] W. Han and M. Sofonea, "Evolutionary variational inequalities arising in viscoelastic contact problems," *SIAM Journal on Numerical Analysis*, vol. 38, no. 2, pp. 556–579, 2001.
- [13] B. Awbi, O. Chau, and M. Sofonea, "Variational and numerical analysis for a frictional contact problem for viscoelastic bodies," *International Mathematical Journal*, vol. 1, pp. 333–348, 2002.
- [14] W. Han and M. Sofonea, *Quasistatic Contact Problems in Viscoelasticity and Viscoplasticity*, Studies in Advanced Mathematics 30, AMS-IP, American Mathematical Society, International Press, Somerville, Mass, USA, 2002.
- [15] M. Campo, J. R. Fernández, and J. M. Viaño, "Numerical analysis and simulations of a quasistatic frictional contact problem with damage in viscoelasticity," *Journal of Computational & Applied Mathematics*, vol. 192, no. 1, pp. 30–39, 2006.
- [16] F. F. Mahmoud, A. G. El-Shafei, and M. A. Attia, "An incremental adaptive procedure for viscoelastic contact problems," *Journal of Tribology*, vol. 129, no. 2, pp. 305–313, 2007.
- [17] F. F. Mahmoud, A. G. El-Shafei, A. E. Al-Shorbagy, and A. A. Abdel-Rahman, "A numerical solution for quasistatic viscoelastic frictional contact problems," *Journal of Tribology*, vol. 130, no. 1, pp. 1–13, 2008.
- [18] P. Wriggers, *Computational Contact Mechanics*, Springer, Berlin, Germany, 2nd edition, 2006.
- [19] F. P. Bowden and D. Tabor, *Friction: An Introduction to Tribology*, Heinemann Mooks, London, UK, 1973.
- [20] W. W. Tworzydlo, W. Cecot, J. T. Oden, and C. H. Yew, "Computational micro- and macroscopic models of contact and friction: formulation, approach and applications," *Wear*, vol. 220, no. 2, pp. 113–140, 1998.
- [21] J. T. Oden and E. B. Pires, "Nonlocal and nonlinear friction laws and variational principles for contact problems in elasticity," *Journal of Applied Mechanics*, vol. 50, no. 1, pp. 67–76, 1983.
- [22] J. T. Oden and E. B. Pires, "Algorithms and numerical results for finite element approximations of contact problems with non-classical friction laws," *Computers & Structures*, vol. 19, no. 1–2, pp. 137–147, 1984.
- [23] K. L. Johnson, *Contact Mechanics*, Cambridge University Press, Cambridge, UK, 1985.
- [24] M. J. Jaffar, "Asymptotic behaviour of thin elastic layers bonded and unbonded to a rigid foundation," *International Journal of Mechanical Sciences*, vol. 31, no. 3, pp. 229–235, 1989.
- [25] J. R. Barber, "Contact problems for the thin elastic layer," *International Journal of Mechanical Sciences*, vol. 32, no. 2, pp. 129–132, 1990.
- [26] M. Teodorescu, H. Rahnejat, R. Gohar, and D. Dowson, "Harmonic decomposition analysis of contact mechanics of bonded layered elastic solids," *Applied Mathematical Modelling*, vol. 33, no. 1, pp. 467–485, 2009.
- [27] G. R. Naghieh, Z. M. Jin, and H. Rahnejat, "Contact characteristics of viscoelastic bonded layers," *Applied Mathematical Modelling*, vol. 22, no. 8, pp. 569–581, 1998.
- [28] G. R. Naghieh, H. Rahnejat, and Z. M. Jin, "Characteristics of frictionless contact of bonded elastic and viscoelastic layered solids," *Wear*, vol. 232, no. 2, pp. 243–249, 1999.
- [29] M. J. Jaffar, "A numerical investigation of the sinusoidal model for elastic layers in line contact," *International Journal of Mechanical Sciences*, vol. 39, no. 5, pp. 497–506, 1997.
- [30] M. J. Jaffar, "Effect of friction on subsurface stresses in sliding line contact of multilayered elastic solids," *International Journal of Solids and Structures*, vol. 37, no. 44, pp. 6571–6575, 2001.

- [31] M. J. Jaffar, "The effect of sinusoidal roughness profile upon rolling plane layered contact," *Tribology International*, vol. 34, no. 3, pp. 171–180, 2001.
- [32] I. Goryacheva and F. Sadeghi, "Contact characteristics of a rolling/sliding cylinder and a viscoelastic layer bonded to an elastic substrate," *Wear*, vol. 184, no. 2, pp. 125–132, 1995.
- [33] I. Goryacheva, F. Sadeghi, and G. Xu, "Viscoelastic effects in lubricated contacts," *Wear*, vol. 198, no. 1-2, pp. 307–312, 1996.
- [34] L.-J. Xiao, X.-H. Sui, and D.-J. Miao, "Study on mechanics of driving drum with superelastic convexity surface covering-layer structure," *Journal of Bionic Engineering*, vol. 5, supplement 1, pp. 60–65, 2008.
- [35] M. L. Williams, "Structural analysis of viscoelastic materials," *AIAA Journal*, vol. 2, no. 5, pp. 785–808, 1964.
- [36] M. M. Hassan and F. F. Mahmoud, "A generalized adaptive incremental approach for solving inequality problems of convex nature," *Structural Engineering & Mechanics*, vol. 18, no. 4, pp. 461–474, 2004.
- [37] J. Dunders, *Properties of Elastic Bodies in Contact*, Delft University Press, Delft, The Netherlands, 1974.
- [38] R. A. Schapery, "Viscoelastic behavior and analysis of composite materials," in *Mechanics of Composite Materials*, G. P. Sendekyj, Ed., pp. 85–168, Academic Press, New York, NY, USA, 1974.
- [39] E. Rabinowicz, *Friction and Wear of Materials*, John Wiley & Sons, New York, NY, USA, 1995.
- [40] K. J. Bathe, *Finite Element Procedures*, Prentice-Hall, Upper Saddle River, NJ, USA, 1996.
- [41] S. A. Mohamed, M. M. Helal, and F. F. Mahmoud, "An incremental convex programming model of the elastic frictional contact problems," *Structural Engineering & Mechanics*, vol. 23, no. 4, pp. 431–447, 2006.

